PLUTONIC TO VOLCANIC ROCKS OF THE VOYKAR OPHIOLITE MASSIF (POLAR URALS): STRUCTURAL AND GEOCHEMICAL CONSTRAINTS ON THEIR ORIGIN

A.A. Saveliev*, **A.Ja. Sharaskin*** and **M. D'Orazio****

* *Geological Institute, Russian Academy of Science, Pyzhevskii per. 7, Moscow, 109017 Russia.*

** *Dipartimento di Scienze della Terra, Università di Pisa, Via S. Maria 53, 56126 Pisa, Italy (dorazio@dst.unipi.it).*

Keywords: *Voykar ophiolites, geochemistry, subduction-related magmas, inter-arc basin, Silurian-Devonian. Polar Urals*

ABSTRACT

Tectonised mantle ultramafic rocks constituting the major part of theVoykar ophiolite massif are intruded by two rock series: (1) the Trubaju complex (mainly pyroxenites and norites), and (2) the Izshor complex (mainly gabbros, diabases and troctolites). The Trubaju rocks were emplaced earlier and at deeper levels with respect to the Izshor ones.

Geochemical criteria, such as the relative REE, HFSE and LILE abundances and major-element variations, suggest that the rocks from both these complexes crystallised from magmas very similar in many geochemical parameters, originating from a highly depleted mantle source. The studied rocks are extremely depleted in Y, Zr, Hf and Nb as compared to normal MORB, thus their parental magmas can be interpreted as generated in supra-subduction environments of an inter-arc basin that split an older island-arc structure during the Early Devonian.

The existence of the basin was short, and prior to the Eifelian; relic fragments of the basin crust were emplaced as the Voykar allochthonous ophiolite into the composite arc structure whose tectonic evolution terminated in the Late Devonian prior to its collision with the continental margin of the East European platform.

INTRODUCTION

The Voykar ophiolite massif is the most spectacular and, in many respects, the best studied within the Polar Urals region. According to available descriptions and interpretations (Dobretsov et al., 1977; Saveliev and Savelieva, 1977; Saveliev and Samygin, 1979; Perfiliev, 1979; Savelieva,1987; Savelieva and Saveliev, 1992; Savelieva and Nesbitt, 1996; Saveliev, 1997), the Uralide structure of the region consists of a series of tectonic nappes sequentially stacked and thrust westward over the edge of the East European platform (Fig. 1).

The Voykar zone (comprising Voykar, Syumkeu and Rayiz massifs) is wedged between the Tagil and Voykar-Shchuch'ya island arc units. The westernmost boundary of the Voykar zone is marked by rock exposures of the "ophiolitic metamorphic sole" (garnet-zoisite amphibolites with relict gabbroic textures) overlying both rocks of the Tagil zone and the thrust stack of the continental slope and shelf deposits. This stack is subdivided, from east to west, into the Salatim (black shales, cherts, tholeiitic basalts), Uraltau (rift-type volcanics and sediments), Lemva (deep-shelf sediments), and Eletsk (shallow-shelf carbonate and siliciclastic deposits) zones. The continental margin and slope deposits, whose basal conglomerates lie unconformably on the Late Precambrian-Early Cambrian basement of the European plate, are believed to characterise a progressive deepening of the margin toward the east, showing an intricate development after the start of the Late Cambrian-Early Ordovician rift stage during which volcanic and sedimentary rocks of the Uraltau zone originated (Savelieva and Nesbitt, 1996; Saveliev, 1997).

All tectonic zones of the European continental margin are separated from rocks of the oceanic domains by a narrow blueschist belt. The Tagil zone consists of island-arc calc-alkaline lavas, tuffs, volcaniclastic and subordinate marine sediments spanning the stratigraphic range from Early Silurian to Middle Devonian. The same age interval is characteristic of the Voykar-Shchuch'ya island arc, located east of the Voykar ophiolite zone. This island-arc domain incorporates a belt of tonalite-diorite intrusions and a volcanic rock sequence intercalated with marine and clastic sediments, including polymict coarse- to fine-grained siliciclastic varieties (Yazeva and Bochkarev,1984). The Voykar-Shchuch'ya sequence is assumed to overlie an oceanic association of diabase dike swarms and pillow lavas interlayered with red jaspery beds. In an area adjacent to the northern termination of the Voykar massif, these rocks, presumably representing the oceanic basement of the Silurian-Mid-Devonian island arc, are exposed very close to an isolated outcrop of limestone, initially dated back to the Ordovician (Lupanova and Markin, 1964); however, later finds of Silurian-Early Devonian macrofauna (crinoids and amphipores, personal communication by L.Ya. Ostrovsky) made the age interpretation ambiguous.

It should be stressed that pillow lava units are missing from all ophiolite massifs of the Voykar zone, although dike swarms or fragments of sheeted dike complexes are commonly found. On the basis of limited geochemical data, the dikes of the massifs are thought to be of MORB affinity (Yazeva and Bochkarev, 1984). Their age is defined as approximately corresponding to 387 ± 34 Ma (the Sm-Nd whole-rock "isochron" for a series of ultramafic and mafic rocks from the Voykar massif, Sharma et al., 1995). This Early Devonian date is obviously discordant with the inferred starting time of the aforementioned rifting stage in the development of the northern Uralides, as well as with the suggested Ordovician age of the oceanic basement of the Voykar-Shchuch'ya and, apparently, of the Tagil island arcs.

This age discrepancy and the peculiar structural position of the Voykar zone show that the North Uralian ophiolites can hardly be interpreted as relic fragments of Early Paleozoic oceanic crust originating in a previous mid-ocean

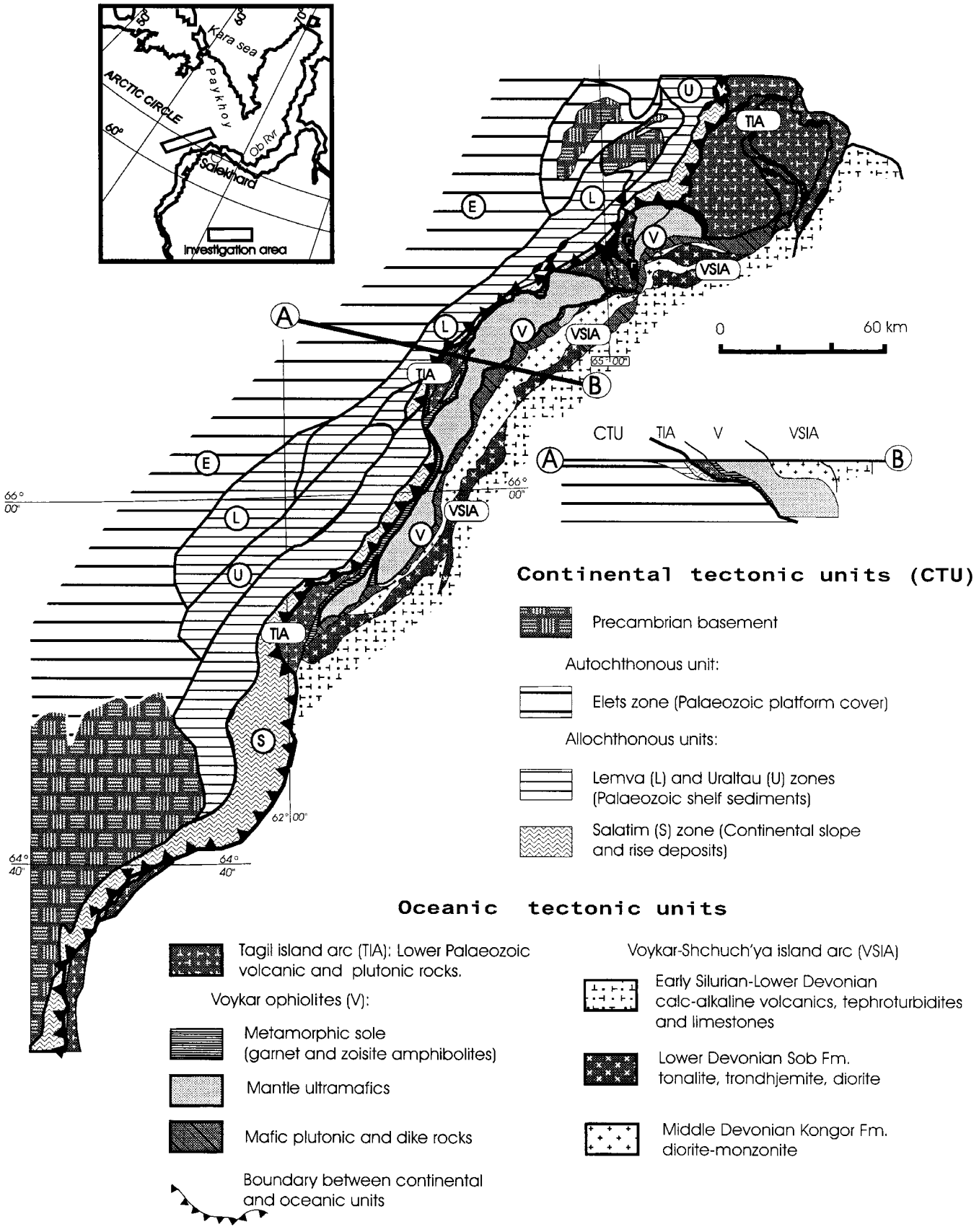

Fig. 1 - Geological map of the Polar Urals showing the structural setting of the Voykar ophiolite.

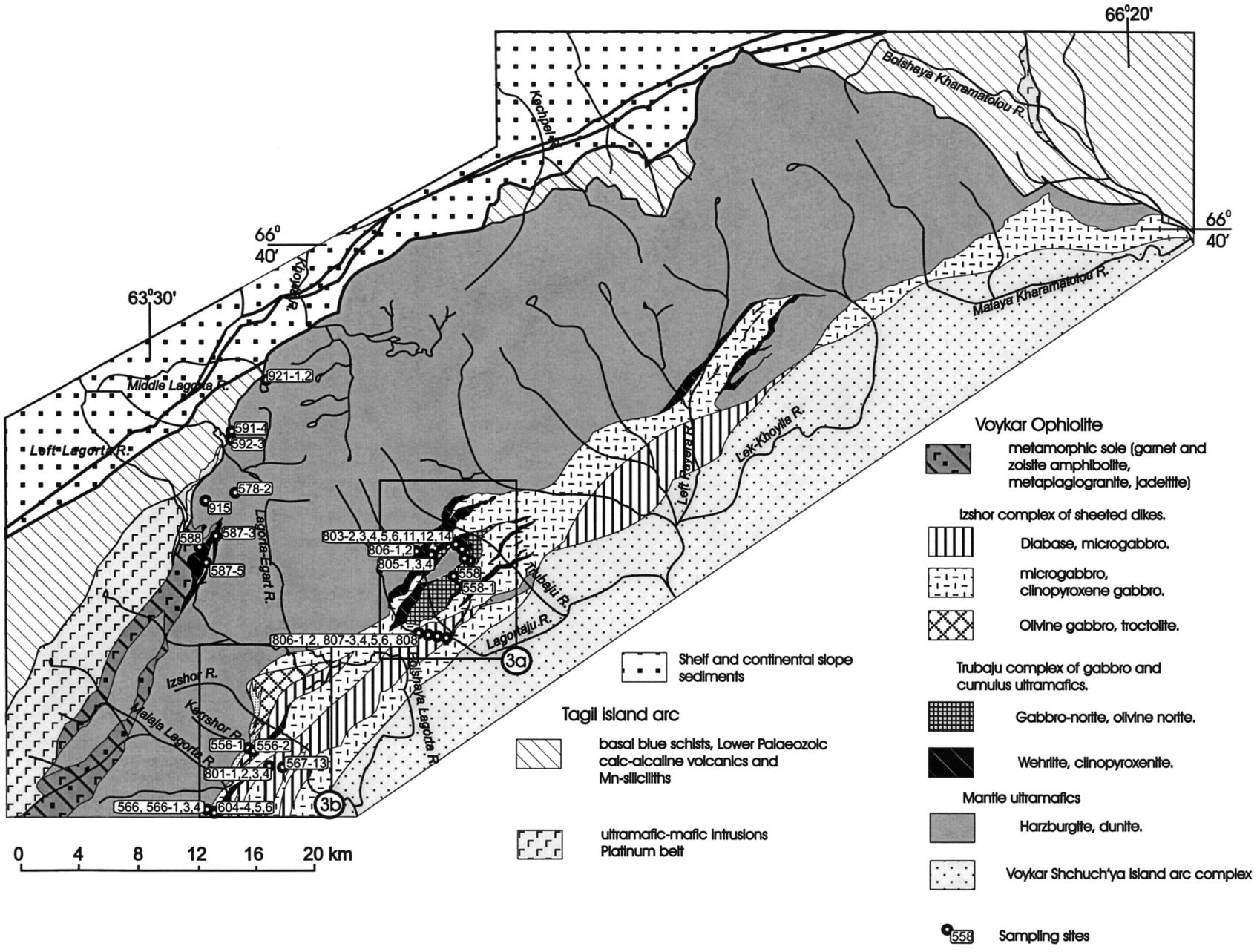

Fig. 2 - Geological sketch map showing the sampling sites of the studied rocks. Rectangles enclose the enlarged areas of Fig. 3.

ridge setting. In order to better understand their origin, we focused our attention on the comprehensive geochemical analysis of plutonic and dike rocks of the Voykar massif and on the geological relationships between these rocks, as well as between the massif itself and surrounding tectonic zones.

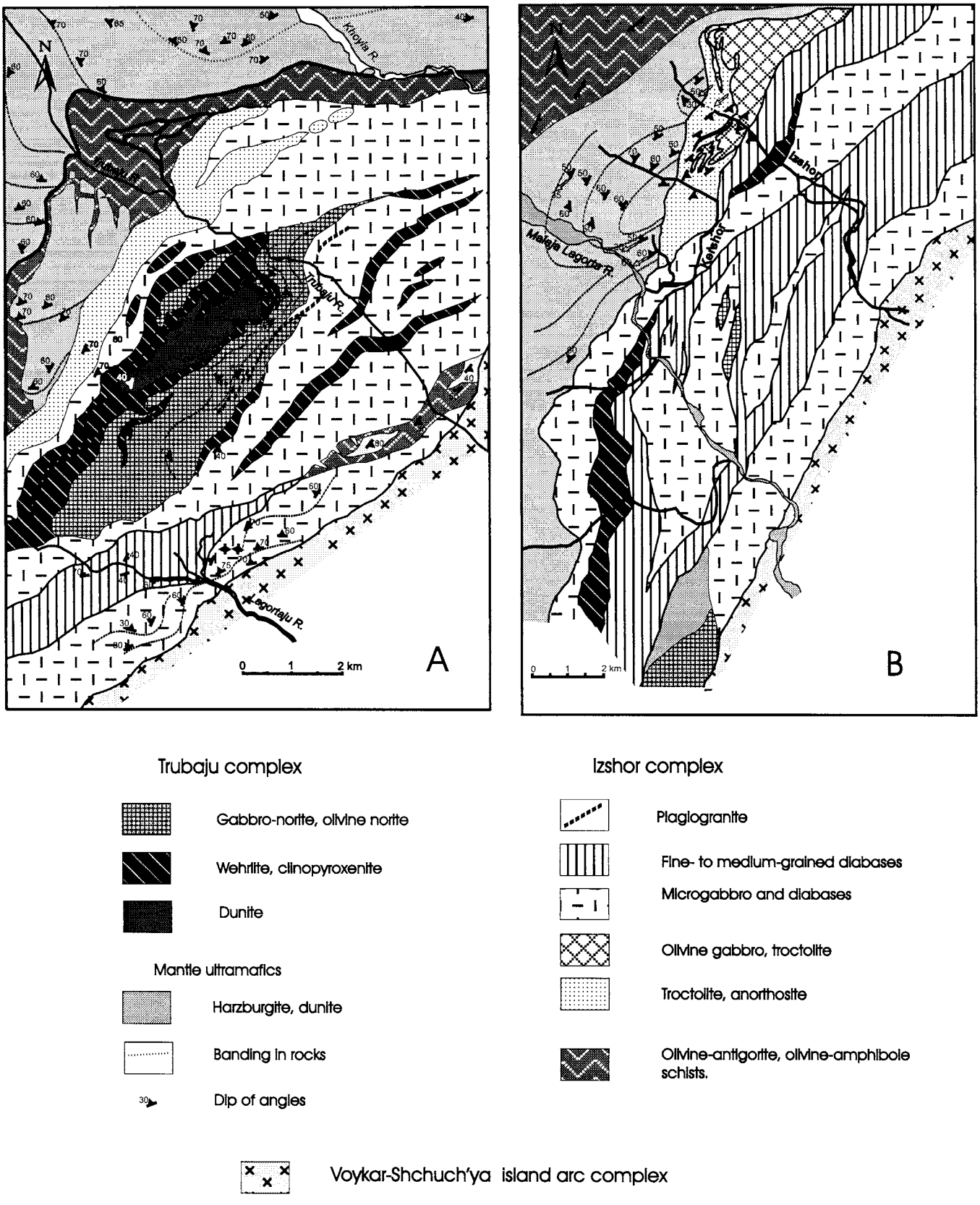

Fig. 3 - Geological sketch maps for the areas surrounding the rivers Trubaju (A) and Izshor (B),illustrating the relations between rock complexes of the Voykar ophiolite massif. Note that rocks of the Izshor complex crosscut the ultramafic mantle tectonites, the rocks of Trubaju complex, and antigorite-olivine and amphibole-olivine schists, locally constituting screens between dikes (rocks of both complexes crop out in both the areas depicted in Fig. 3A and 3B).

Table 1 - Petrographic synopsis for the studied magmatic rocks from the Voykar ophiolite.

Rock types	Textures	Mineral assemblages	Composition of minerals	Alteration (secondary minerals)
T r u b a j u c o m p l e x				
dunite	coarse-grained, granular	olivine + spinel	olivine (Fo $_{85-92}$)	chrysotile + magnetite (≤ 80%) after olivine
wehrlite	coarse-grained, glomerophyric to poikilitic	olivine + clinopyroxene + spinel	olivine (Fo $_{\leq 16,5}$)	chrysotile + magnetite (≤ 80%) after olivine amphibole + chlorite (≤ 40%) after clinopyroxene
clinopyroxenite	coarse-grained, glomerophyric to pegmatoid	olivine + clinopyroxene ± magnetite	olivine (Fo $_{\leq 18,7}$)	chrysotile + magnetite (≤ 80%) after olivine amphibole + chlorite (≤ 40%) after clinopyroxene
norite	medium to coarse-grained, hypidiomorphic-granular	olivine + orthopyroxene + clinopyroxene + plagioclase + hornblende ± magnetite	olivine (Fo $_{\leq 28}$) orthopyroxene (Fs $_{25-36}$) clinopyroxene(Fs $_{22-33}$) plagioclase (An $_{60-90}$)	serpentine + bastite (≤40%) after olivine and orthopyroxene amphibole + chlorite (≤40%) after clinopyroxene
I z s h o r c o m p l e x				
diabase-microgabbro (dikes)	microophitic, ophitic, poikilophitic, porphyritic	plagioclase + clinopyroxene	plagioclase (An $_{36-70}$)	amphibole + chlorite + albite aggregate (≤10-90%) after primary minerals
olivine gabbro (screens between and root zone of the dikes)	medium to coarse-grained to hypidiomorphic-granular	olivine + clinopyroxene + plagioclase	plagioclase (An $_{40-65}$)	amphibole + chlorite + albite aggregate (≤40-90%) after primary minerals
gabbro-pegmatite	coarse-grained pegmatitic	plagioclase + amphibole ± clinopyroxene	plagioclase (An $_{20-30}$)	amphibole + chlorite + albite aggregate (≤20-90%) after primary minerals
troctolite (aureole)	medium to coarse-grained, glomerophyric, poikylitic	olivine + orthopyroxene + clinopyroxene + plagioclase	olivine (Fo $_{75-85}$) plagioclase (An $_{80-90}$)	serpentine + bastite (≤40%) after olivine and orthopyroxene amphibole + chlorite (≤40%) after clinopyroxene zoisite + saussurite(≤80%) after plagioclase

Table 2 - Major- and trace-element analyses for representative magmatic rocks from the Voykar ophiolite massif.

	Trubaju complex												Izshor complex													Voykar-Shchuch'ya	
Sample	556-2	558	558-1	567-13	578-2	801-2	803-2	803-14	587-3	587-5	588	591-4	604-4	604-5	604-6	807-3	801-1	801-3	807-4	807-5	807-6	921-1	556-1	808	901-2	806-1	605-1	605-2
Rock type	Norite	Norite	Norite	Norite	Norite	Norite	Norite	Norite	Cpx.te	Cpx.te	Cpx.te	Wehrlite	Diabase	Diabase	Diabase	Diabase	Micro-G	Micro-G	Micro-G	Micro-G	Micro-G	Micro-G	Micro-G	G-Peg	Gabbro	Mela-G	Bas. And.	Andesite
SiO_2 (wt%)	47,15	44,65	46,74	44,09	45,73	47,68	46,81	46,88	48,98	50,90	49,90	40,94	45,50	50,02	45,85	50,01	45,01	54,81	50,07	50,68	45,77	46,76	48,90	44,30	46,88	42,21	54,25	57,80
TiO_2	0,26	0,34	0,19	0,45	0,26	0,64	0,40	0,29	0,16	0,17	0,16	0,21	0,45	1,94	0,41	0,85	0,36	0,47	0,79	1,66	0,29	0,51	0,47	2,86	0,34	0,17	0,38	0,66
Al_2O_3	8,60	19,64	21,31	13,72	16,96	15,37	17,23	17,54	2,49	0,58	1,29	4,41	19,56	14,26	16,49	14,44	15,41	15,78	13,23	14,00	19,22	17,77	12,56	17,75	17,71	8,62	15,19	14,13
Fe_2O_3	4,78	1,00	1,52	1,79	3,07	2,40	2,44	2,23	3,24	2,53	2,79	5,14	2,33	6,38	4,04	4,41	2,08	2,66	5,05	6,51	4,62	1,97	2,65	0,01	4,44	3,18	2,00	3,19
FeO	6,17	5,24	5,45	5,88	3,34	6,91	8,18	7,22	4,84	4,70	3,54	4,48	3,09	4,54	6,65	6,08	5,53	6,25	8,37	8,45	2,49	3,20	7,72	8,76	2,86	3,56	7,90	7,54
MnO	0,11	0,11	0,21	0,14	0,12	0,10	0,13	0,26	0,09	0,10	0,10	0,10	0,10	0,24	0,19	0,15	0,06	0,03	0,19	0,18	0,09	0,09	0,14	0,17	0,08	0,14	0,15	0,16
MgO	20,24	10,60	10,58	15,19	13,09	10,76	9,84	10,21	18,04	19,58	20,64	32,58	8,82	4,94	8,76	8,05	11,89	5,84	6,34	4,56	8,00	11,02	10,77	1,47	8,23	25,82	6,35	4,24
CaO	10,17	15,09	12,66	13,14	14,65	14,07	13,45	14,43	18,55	20,31	19,48	6,21	16,98	9,19	14,26	12,21	15,48	9,29	10,09	8,60	14,89	12,13	12,77	18,32	15,63	9,87	5,33	4,21
Na_2O	0,58	0,68	0,68	1,66	1,30	1,29	0,78	0,58	0,52	0,45	0,45	0,60	1,00	3,77	0,54	2,60	0,84	2,28	3,07	4,62	1,98	3,49	1,77	3,43	1,59	0,58	4,02	3,85
K_2O	0,09	0,06	0,06	0,13	0,09	0,06	0,06	0,06	0,07	0,05	0,06	0,10	0,02	0,91	0,06	0,15	0,13	0,13	0,49	0,25	0,18	0,59	0,13	0,05	0,06	0,06	0,25	0,09
P_2O_5	<d.l.	<d.l.	<d.l.	<d.l.	<d.l.	<d.l.	<d.l.	<d.l.	<d.l.	<d.l.	<d.l.	<d.l.	0,02	0,87	0,01	<d.l.	<d.l.	0,08	0,01	0,02	<d.l.	<d.l.	<d.l.	0,01	<d.l.	<d.l.	0,04	0,06
LOI	2,09	2,06	0,50	3,66	0,90	0,64	0,91	0,68	2,58	0,97	1,64	4,82	2,33	1,52	2,31	0,62	2,49	2,03	2,10	0,46	1,72	2,13	1,76	3,18	2,03	5,84	3,96	4,08
Total	100,24	99,47	99,90	99,85	99,51	99,92	100,24	100,38	99,56	100,35	100,06	99,59	100,20	98,58	99,57	99,57	99,29	99,65	99,80	99,99	99,25	99,66	99,64	100,31	99,85	100,05	99,82	100,02
H_20+	1,83	1,89	0,39	n.d.	n.d.	0,51	n.d.	0,55	n.d.	n.d.	n.d.	n.d.	1,77	n.d.	0,31	0,44	2,37	1,42	1,87	0,34	1,45	n.d.	1,61	1,68	1,88	5,32	n.d.	n.d.
Mg#	79,6	77,7	75,8	80,4	81,3	70,6	65,7	69,1	82,5	85,0	87,3	87,9	77,5	49,3	63,3	61,8	76,5	57,7	49,8	39,2	70,9	81,8	68,3	25,3	70,8	89,1	57,0	45,2
Rb (ppm)	0,10	0,16	0,08	1,67	1,38	0,06	0,14	0,09	0,10	0,08	0,09	n.d.	0,30	13,3	1,00	0,44	n.d.	n.d.	4,0	0,43	0,33	2,41	0,11	0,47	0,23	0,04	1,92	0,21
Sr	50	104	158	55	154	122	104	100	8,9	5,3	12,6	n.d.	137	389	154	169	160	99	662	162	135	115	42	295	121	39	142	37
Y	1,49	1,25	0,39	6,1	4,7	8,3	1,99	1,51	2,66	0,99	1,70	n.d.	5,2	43	2,53	15,8	n.d.	n.d.	16,7	33	2,95	11,4	5,8	9,9	3,9	2,01	14,3	20,8
Zr	7,7	0,53	0,26	1,52	2,44	9,1	0,51	0,53	0,47	0,61	0,82	n.d.	4,9	210	1,40	15,8	n.d.	n.d.	66	44	2,04	6,1	11,6	5,6	1,96	1,14	24,2	39
Nb	<d.l.	<d.l.	<d.l.	<d.l.	<d.l.	0,03	<d.l.	<d.l.	<d.l.	<d.l.	<d.l.	n.d.	0,05	7,7	<d.l.	0,60	n.d.	n.d.	1,76	1,33	0,02	0,04	0,08	0,58	0,01	<d.l.	0,29	0,31
Cs	0,05	<d.l.	<d.l.	0,24	0,02	<d.l.	0,02	<d.l.	0,03	<d.l.	0,04	n.d.	<d.l.	0,17	0,02	<d.l.	n.d.	n.d.	0,07	<d.l.	<d.l.	0,03	0,01	0,02	0,03	<d.l.	0,12	0,04
Ba	0,42	4,7	1,13	2,84	88	2,19	1,70	0,50	1,97	0,57	1,69	n.d.	5,1	278	10,6	22,5	n.d.	19,0	152	25,5	11,0	75	1,85	12,3	3,7	0,47	41	7,7
Hf	0,17	0,03	0,01	0,11	0,13	0,29	0,02	0,02	0,03	0,02	0,04	n.d.	0,21	5,1	0,06	0,77	n.d.	n.d.	2,04	1,61	0,09	0,38	0,40	0,27	0,10	0,07	0,92	1,37
La (ppm)	0,02	0,01	0,02	0,34	0,11	0,37	0,04	<d.l.	0,02	<d.l.	<d.l.	n.d.	0,28	20,6	0,14	1,69	0,19	0,65	17,4	3,7	0,12	0,22	0,76	0,37	0,23	0,25	1,22	1,83
Ce	0,08	0,05	0,06	0,46	0,38	1,43	0,11	0,03	0,11	<d.l.	0,07	n.d.	0,91	54	0,39	5,3	0,56	1,80	38	11,8	0,38	0,86	2,29	1,14	0,62	0,56	3,6	5,8
Pr	0,02	0,01	0,01	0,07	0,07	0,28	0,02	0,01	0,03	<d.l.	0,02	n.d.	0,18	7,7	0,07	0,89	n.d.	n.d.	4,9	2,00	0,08	0,21	0,38	0,22	0,10	0,07	0,58	0,95
Nd	0,12	0,12	0,06	0,54	0,55	1,77	0,14	0,11	0,23	0,05	0,16	n.d.	1,05	37	0,37	5,1	0,60	1,50	21,3	10,9	0,56	1,51	2,11	1,55	0,69	0,35	3,1	5,5
Sm	0,07	0,08	0,02	0,32	0,32	0,81	0,10	0,06	0,15	0,06	0,11	n.d.	0,49	9,1	0,20	1,75	0,25	0,63	4,8	3,7	0,25	0,89	0,66	0,79	0,30	0,15	1,27	2,09
Eu	0,06	0,08	0,05	0,22	0,20	0,39	0,13	0,10	0,10	0,03	0,05	n.d.	0,30	3,3	0,09	0,73	0,13	0,26	1,26	1,31	0,16	0,48	0,29	0,71	0,24	0,10	0,53	0,77
Gd	0,15	0,14	0,03	0,76	0,66	1,07	0,21	0,13	0,38	0,12	0,21	n.d.	0,70	9,1	0,35	2,21	n.d.	n.d.	3,9	4,4	0,47	1,44	0,90	1,36	0,60	0,30	1,67	2,50
Tb	0,04	0,03	0,01	0,15	0,11	0,22	0,05	0,03	0,07	0,03	0,04	n.d.	0,15	1,47	0,06	0,43	0,07	0,26	0,52	0,94	0,09	0,32	0,15	0,27	0,12	0,06	0,37	0,54
Dy	0,25	0,21	0,06	1,05	0,77	1,40	0,36	0,25	0,51	0,19	0,32	n.d.	0,91	8,1	0,46	2,60	n.d.	n.d.	2,85	5,5	0,60	1,98	1,03	1,79	0,75	0,36	2,28	3,4
Ho	0,06	0,05	0,02	0,24	0,17	0,32	0,09	0,06	0,11	0,04	0,07	n.d.	0,21	1,75	0,11	0,60	n.d.	n.d.	0,64	1,23	0,13	0,45	0,22	0,40	0,17	0,08	0,57	0,84
Er	0,19	0,15	0,05	0,72	0,48	0,90	0,23	0,17	0,34	0,12	0,19	n.d.	0,59	4,3	0,33	1,70	n.d.	n.d.	1,65	3,6	0,42	1,28	0,67	1,10	0,47	0,24	1,63	2,36
Tm	0,03	0,02	0,01	0,10	0,07	0,14	0,04	0,04	0,05	0,02	0,03	n.d.	0,09	0,65	0,06	0,27	n.d.	n.d.	0,26	0,55	0,05	0,20	0,10	0,16	0,07	0,03	0,28	0,39
Yb	0,25	0,13	0,07	0,64	0,45	0,89	0,27	0,23	0,29	0,11	0,17	n.d.	0,51	4,0	0,38	1,64	0,26	1,10	1,64	3,7	0,36	1,26	0,61	1,00	0,41	0,18	1,71	2,47
Lu	0,04	0,02	0,01	0,10	0,06	0,13	0,04	0,04	0,04	0,02	0,02	n.d.	0,08	0,57	0,06	0,24	0,04	0,18	0,23	0,51	0,05	0,16	0,09	0,15	0,06	0,03	0,26	0,37

Note: <d.l. = below detenction limit; n.d. = not determined; Bas. And. = basaltic andesite; Cpx.te = clinopyroxenite; Micro-G = microgabbro; G-Peg = gabbro-pegmatite; Mela-G = mela-gabbro; Mg# = Mg/(Mg+Fe") assuming Fe_2O_3/FeO (wt%) = 0.15

GEOLOGICAL SETTING OF THE STUDIED ROCK SAMPLES.

Geological characteristics of the Voykar massif have already been described in detail in several publications (e.g., Savelieva, 1987), and here we shall recall only the principal features relevant for the subsequent discussion. Most of the massif (Fig. 2) is composed of tectonised mantle ultramafics (harzburgites and dunites). This huge allochthonous body of ultramafic rocks (up to 200 km long, about 20-30 km wide, and more than 4 km thick) is intruded by two rock series: (1) the Trubaju Complex of wehrlite, clinopyroxenite and norite, and (2) the Izshor Complex of sheeted diabase and microgabbro dikes associated with minor intrusive bodies of gabbro and troctolite-gabbro-anorthosite aureoles at the contact with mantle ultramafics (Fig. 2 and 3). Both complexes are most clearly developed along the south-eastern periphery of the massif (Fig. 2), where Saveliev (1997) established the following geological and genetic relationships between the rocks. The Trubaju rock series apparently originated during fractional crystallisation of high-Mg basaltic magma in a chamber surrounded by hot harzburgite masses, as can be deduced from the lack of any sign of magma chilling against harzburgites. The isolated harzburgite blocks within the Trubaju rocks and irregular, often interfingering contacts between the former and the latter (Fig. 3A) are interpreted as the result of the dynamic interaction between the magma chamber and host mantle rocks. Contacts between various rock types of the Trubaju complex are of the same kind, and again suggest the unstable tectonic environments of magma emplacement and crystallisation. In general, this complex resembles the layered ultramafic-mafic units of classical ophiolite sequences (Anonymous, 1972; Nicolas, 1989); however, layering in this case is extremely irregular, frequently vague and intermittent along the strike (Fig. 3A).

The Izshor Complex crosscuts both the ultramafic mantle tectonites and theTrubaju Complex (Fig. 2 and 3). Dike swarms and sheeted dikes of clinopyroxene, olivine and amphibole microgabbro and diabases are the most characteristic rock types of the complex. Apparently, there are several generations of dikes. Ensembles of sheeted dikes with one chilled margin are somewhat older than dike swarms and isolated dikes with two chilled margins, which cut these ensembles and frequently display plagiophyric textures. Linear and lenticular zones of fine- to medium-grained diabase dikes (few hundreds of meters to one-two kilometres wide) intricately alternate with similar zones of coarser-grained microgabbro and gabbro dikes (Fig. 3). In both zones, the dikes are steeply dipping and strike subparallel to the elongation of the massif. Screen rocks of the dike complex are represented by either mantle harzburgites and dunites, or norites and pyroxenites of the Trubaju Complex, as well as by olivine to clinopyroxene gabbros, troctolites and anorthosites lacking in the last complex. Close to the contact with the ultramafic core of the Voykar massif, dikes crosscut the troctolite-gabbro-anorthosite rock association (Fig. 3B).Within such local zones, olivine gabbros engulf the rootless microgabbro and diabase dikes, and locally grade into blurry distribution areas of troctolite-anorthosite association. Dichotomous bodies of melagabbro or anorthosite pierce into the mantle ultramafics in a form of diffuse aureole surrounded by a blurred zone of troctolites, whose veins locally penetrate into dunite bodies of mantle restites. These relations are interpreted as characteristic aureoles generated by magma injections into the host mantle rocks.

In general, the formation stage of the Izshor complex occurred after a dynamometamorphic event that affected the mantle domain and produced the antigorite-olivine and amphibole-olivine schists locally constituting screens between dikes (Fig. 3). Rock samples for geochemical analysis were collected from well studied outcrops of both rock complexes. Sampling sites are marked on the generalised map of the northern part of the Voykar massif (Fig. 2). Over fifty samples were analysed for major element abundances, and 28 samples of these were selected for trace element analysis. The studied samples represent all the principal varieties of plutonic and dike rocks of the massif. A synopsis of available data on textural features and characteristic mineral assemblages is presented in Table 1.

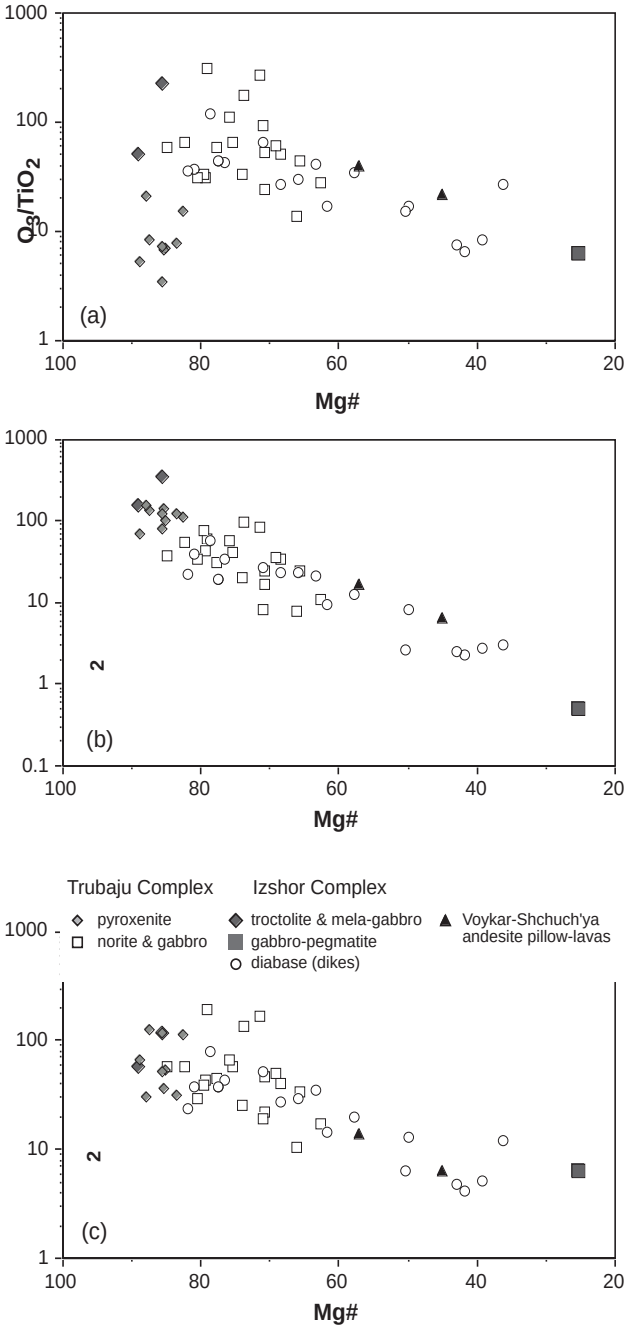

Fig. 4 - Al_2O_3/TiO_2(a), MgO/TiO_2 (b) and CaO/TiO_2 (c) wt% ratios for the Voykar ophiolite rocks plotted against the Mg#. Two andesite pillow-lavas from the Voykar-Shchuch'ya island arc are also plotted for comparison.

ANALYTICAL METHODS

Bulk-rock major-element analyses were performed by classical wet methods at the Geological Institute, Russian Academy of Sciences. The trace elements concentrations were determined by ICP-MS (Fisons PQII+ STE) at the Dipartimento di Scienze della Terra, Università di Pisa, Italy. Rock powders were dissolved by conventional HNO_3 + HF acid digestion (for sample dissolution details see D'Orazio and Tonarini, 1997) and then spiked with Rh, Re and Bi (internal standards). Sample solutions, with a final total dissolved solid < 2 mg ml^{-1} in a 2% (v/v) HNO_3 matrix, were measured with external calibration using well-certified basaltic international reference rocks. ICP-MS measurements were subjected to a correction procedure including blank subtraction, drift-monitoring and oxide-hydroxide isobaric interferences (for REE). All steps of sample preparation were performed in a class 10,000 clean lab. Detection limits (ppm in the solid samples), estimated by calculating the concentration corresponding to 3 times the standard deviation of blank solution counts, range from 0.001 to 0.05 ppm for Y, Nb, Cs and REE, and from 0.05 to 0.5 ppm for Rb, Sr, Zr and Ba. Analytical precision, estimated by repeated analyses of geochemical reference samples, typically ranges from ~10% at 10 x detection limit to 3-5% at 100 x detection limit; consequently, different numbers of significant digits are used to report results. The accuracy of data, evaluated by regularly analysing well-certified geochemical reference samples, typically ranges from 0 to 7% for elements at 50-100 x detection limit.

GEOCHEMICAL CHARACTERISTICS

Representative major- and trace-element analyses are listed in Table 2. The wt% ratios Al_2O_3/TiO_2, MgO/TiO_2 and CaO/TiO_2 versus the Mg#, taken as an index of differentiation, are plotted in Fig. 4. These diagrams involve elements which appear to be the least mobile during secondary rock alteration, and show trends of magmatic fractional crystallisation characterising the Trubaju and Izshor rock series. In Fig. 4a, a clear difference between the plagioclase-free (websterites, clinopyroxenites) and plagioclase-bearing (norites) rocks can be observed. Unexpectedly, Trubaju norites+gabbros plot in all diagrams along the trend characterising the Izshor series of troctolites, microgabbro and diabase dikes. The geochemical similarity of both rock complexes is also suggested, though less clearly, by diagrams of indicative trace elements (Ba, Ce and Zr) plotted versus Mg# (Fig. 5). Chondrite-normalised REE patterns (Fig. 6) do not contradict this conclusion, and variations in abundance of these elements may be well explained, with due regard for the petrographic characteristics of the rocks (Table 1), as depicting REE differentiation in the course of fractional crystallisation of magmas with initially comparable abundances of these elements. Actually, the low absolute REE abundances, LREE depletion and strong positive Eu-anomalies (Eu/Eu* 1.3 - 6.0) are characteristic of the high-Mg low-Ti norites of the Trubaju series, which are rich in cumulus olivine, hypersthene and plagioclase. These features are less pronounced in the more evolved gabbros, whose patterns overlap those characterising the most primitive rocks of the Izshor series (Fig. 6). The evolved gabbro and diabase dikes of the latter series, some of which correspond in composition to basaltic andesites (Table 2), display higher absolute REE abundances and a relative enrichment in LREE. Thus, according to the results of trace- and major-element analysis, we may suspect that the Trubaju and Izshor rocks originated from parental magmas of similar geochemical type, which presumably derived from a common mantle source. Assuming the $(La/Yb)_N$ ratio to be a measure of the mantle depletion degree, for the rocks which are presumably close in composition to parental magmas and intermediate between the cumulate norites and evolved diabase dikes of the Voykar massif, this ratio is within the interval of 0.17-0.39, i.e., less than or comparable to that of primitive MORB (0.34-0.70; Sun et al., 1979). Accordingly, parental magmas originated from a depleted mantle, possibly even more depleted than that below mid-ocean ridges. The diagrams of Fig. 7 show another important feature of the studied rocks, that is, their strong depletion in HFSE (Y, Nb, Zr, Hf). In some samples the concentration of these elements falls by more than two orders of magnitude below the reference abundances in normal MORB (Sun et al., 1979). Some diabase dikes are simultaneously depleted in HFSE and en-

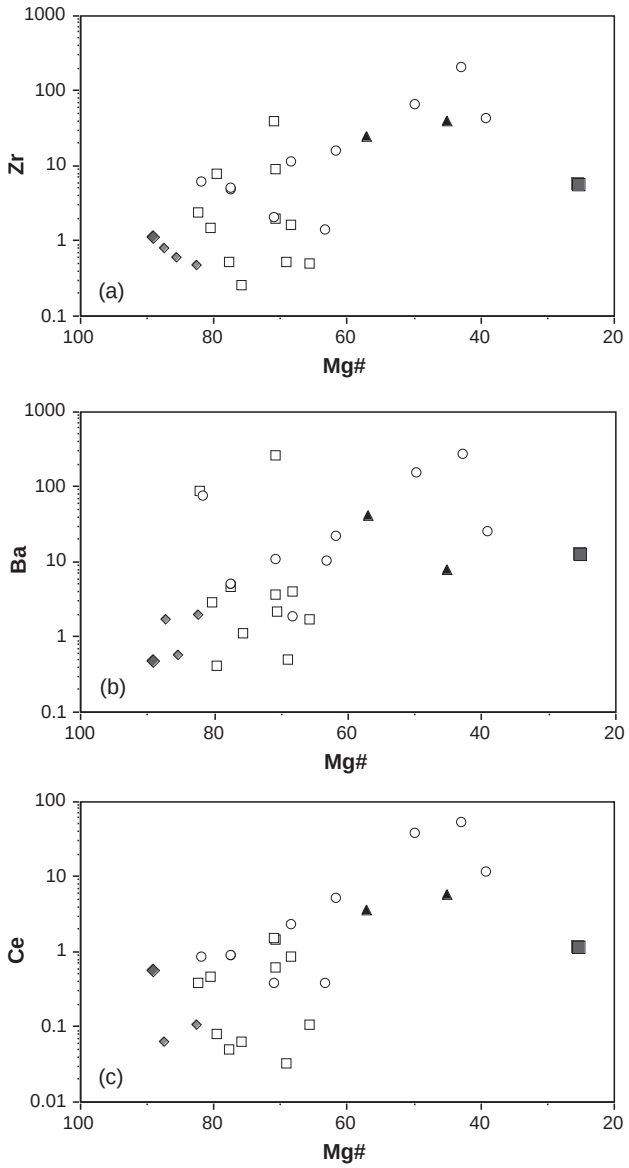

Fig. 5 - Zr (a), Ba (b) and Ce (c) (ppm) for the Voykar ophiolite rocks plotted against the Mg#. Two andesite pillow-lavas from the Voykar-Shchuch'ya island arc are also plotted for comparison. Same symbols as in Fig. 4.

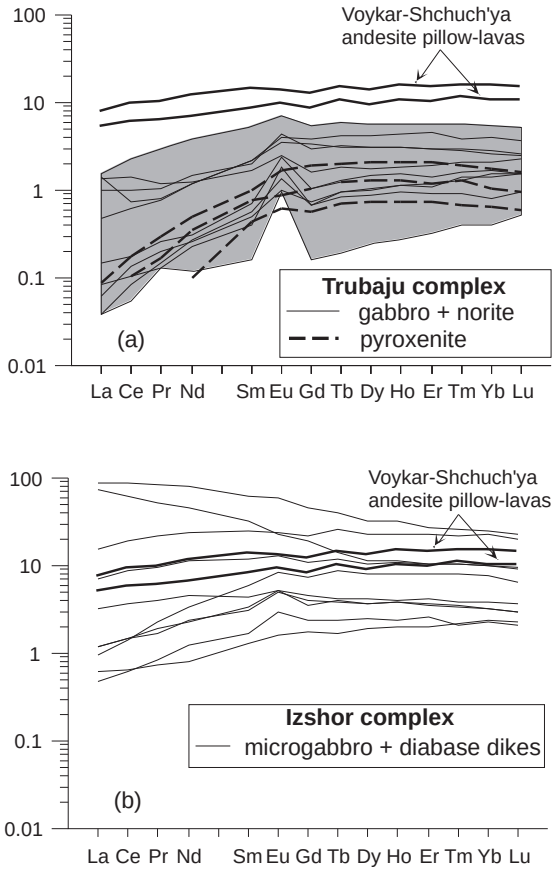

Fig. 6 - Chondrite-normalised REE patterns for Trubaju (a) and Izshor (b) rock series. The greyed are a highlights the field of Trubaju gabbro + norite. REE patterns for the two andesite pillow-lavas from the Voykar-Shchuch'ya island arc are also reported for comparative purposes. Normalising values after Sun and McDonough (1989).

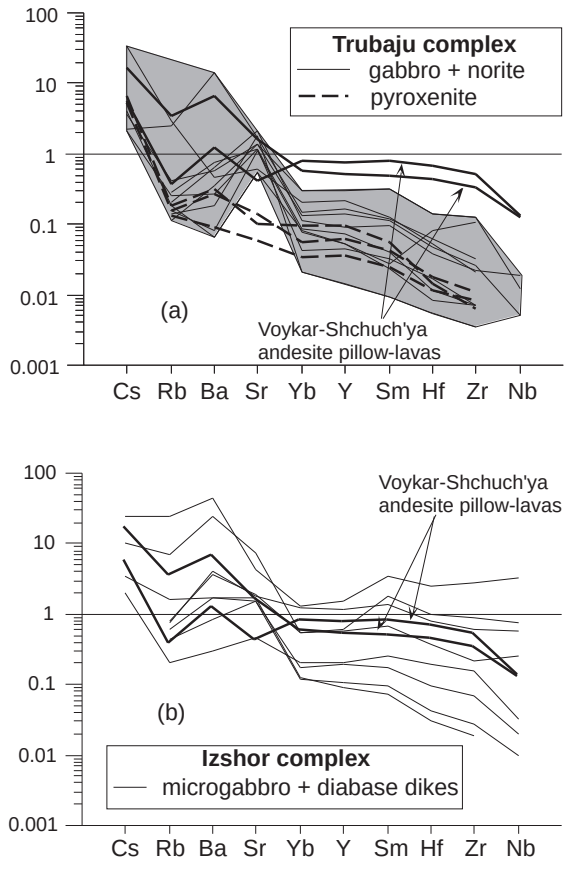

Fig. 7 - N-MORB-normalised diagrams for Trubaju (a) and Izshor (b) rock series. The greyed area highlights the field of Trubaju gabbro + norite. The two andesite pillow-lavas from the Voykar-Shchuch'ya island arc are also reported in both diagrams for comparative purposes. Normalising values after Sun and McDonough (1989).

riched in LILE, especially Cs, Rb, and Ba. This incompatible trace-element distribution is accepted as the diagnostic feature of basic magmas generated in supra-subduction environments (e.g., Pearce et al.,1985). From this viewpoint, it is interesting to note that the two andesitic pillow-lava samples collected from the Voykar-Shchuch'ya island arc zone and analysed for comparison (Table 2), are similar in many geochemical parameters to the low-Mg diabase dikes ofthe Izshor Complex (Tab. 2; Figs. 4-7). The chondrite-normalised REE patterns of these lava samples and their $(La/Yb)_N$ ratio of about 0.5 are close to those of typical normal MORB, but in contrast to these, they are depleted, like the Izshor dikes, in HFSE, especially Zr and Nb (Fig. 7). Thus, parental magmas of these rocks may also have been generated in a supra-subduction setting. Consequently, the samples characterise either an island-arc volcanic complex, or lavas erupted at the floor of an arc-related marginal basin.

DISCUSSION AND CONCLUSIONS

The brief summary of geological data presented above elucidates two important points concerning the origin of plutonic and dike rock complexes of the Voykar ophiolite massif. The data show that the Trubaju complex of dunites, pyroxenites and norites, all displaying coarse granular textures, apparently intruded the host harzburgites at a considerable depth where the mantle rocks were hot enough to preclude magma chilling, and the low thermal gradient favoured slow melt cooling and its fractional crystallisation in the magma chamber. The considerable depth of magmatic injections at this stage can also be inferred from traces of high-T plastic deformations in the mantle harzburgites of the Voykar massif (Savelieva,1987), which presumably concurred in the formation of the Trubaju rocks.

The Izshor Complex originated somewhat later, when harzburgites and rocks of the early intrusive phase rose up and cooled. According to Saveliev (1997), deformations that developed in the mantle domain at this stage are of the semi-brittle and brittle types. Opening fractures served as conduits for magma injections which mostly crystallised in the form of dikes and subvolcanic bodies. It is also possible that some magma chambers of sufficient heat capacity were able to interact at deeper levels with the country rocks and produced the troctolite aureoles and dichotomous veins of olivine gabbro and anorthosites penetrating into the mantle rocks.

The established sequence of magmatic events should now be considered in the light of geochemical results suggesting that parental magmas for the Trubaju and Izshor rocks were similar in geochemical parameters, and might be related to a common melt reservoir in the highly depleted mantle. Indeed, REE analyses of Voykar harzburgites (Sharma et al., 1995) yielded extremely low $(La/Yb)_N$ ratios of about 0.03. Plutonic and dike rocks from the Voykar massif have values of this geochemical parameter lower than in MORB. One of the possible explanations of this geochemical peculiarity is that the time interval between the first and second intrusive phase was rather short. If so, we may certainly consider as

geochronologically meaningful the age of 387 ± 34 Ma estimated by Sharma et al. (1995) on the basis of Sm-Nd isotopic data for a series of whole rock samples which included various plutonic and dike rocks from theVoykar massif. If the dating results can be taken as meaningful, and the mantle, plutonic and dike rocks of the massif can be considered complementary as regards their genetic relationships, then we face the fact that the Voykar ophiolite sequence is considerably younger than the basal Silurian horizons of the island-arc sequences in the Tagil and Voykar-Shchuch'ya zones bordering it to the westand east, respectively. In this a case, the root zone of the Voykar allochthon must be located in the inter-arc basin, but not in the Precambrian (Dobretsov et al., 1977) or Early Palaeozoic (Perfiliev, 1979) Uralian ocean proper. This conclusion is in agreement with the Y, Zr, Hf and Nb depletion of the studied rock samples (Fig. 7). The estimated age of the Voykar sequence may indicate the opening of the postulated inter-arc basin, if the Tagil and Voykar-Shchuch'ya island arcs were conjoined before and represented an integral paleostructure. The suggested tectonic scenario appears quite probable, because both of the island-arc units are in direct contact with one another southwest of the massif (Fig. 1). In addition, the recent results of regional geological observations (unpublished data by Kucherina and Pryamonosov) clearly indicate that sedimentation of the volcanogenic-carbonate type, typical of the Tagil zone, was also dominant in the Shchuch'ya island arc, where the respective geological formations are comparable in age with those of the former zone. Another important point is that the Voykar ophiolites are crosscut by bodies of the tonalite-diorite intrusive belt located southwest of the massif, and xenoliths of ophiolitic rocks, some as wide as several kilometres across, occur within the belt (Saveliev and Savelieva, 1977). According to paleontological dating, the tonalite-diorite belt is pre-Eifelian in age (Lupanova and Markin, 1964; Yazeva and Bochkarev, 1984), this evidence constrains the upper time limit of the inter-arc basin which was a root zone for the ophiolites studied here. If the age obtained by Sharma et al. (1995) is acceptable, then that period was obviously very short, and soon after opening the basin was closed. Its crustal fragments were tectonically emplaced into the island-arc structure and intruded by the tonalite-diorite magma. Problems concerning the subsequent development of the composite Tagil-Voykar-Shchuch'ya island arc are beyond the scope of this paper and have been partially considered in some other publications (Savelieva and Nesbitt, 1996; Saveliev, 1997).

The following main conclusions can be drawn:

1. Geochemical criteria, such as the relative REE, HFSE and LILE abundances suggest that plutonic and dike rocks of the Voykar ophiolites crystallised from magmas very similar in many geochemical parameters, originating in a highly depleted mantle domain above a paleosubduction zone. In terms of REE geochemistry, the domain was apparently much more depleted than the MORB source.

2. The studied rocks are considerably depleted in Y, Zr, Hf and Nb as compared to normal MORB, and their parental magmas must have been generated in supra-subduction environments of an inter-arc basin that split an earlier island-arc structure in the Early Devonian.

3. The basin was short-lived, and, prior to the Eifelian, relic fragments of the basin crust were emplaced as the Voykar ophiolite allochthon into the composite arc structure, whose tectonic evolution terminated in the Late Devonian before its collision with the continental margin of the East European platform.

Acknowledgements

Constructive reviews by E. Saccani and an anonymous reviewer helped to improve the manuscript. This work was financially supported by the Russian Foundation for Basic Research, projects 97-05-64903 and 98-05-64060. The ICP-MS analyses were obtained thanks to "Gruppo Nazionale per la Vulcanologia", C.N.R , Italy.

REFERENCES

Anonymous, 1972. Penrose field conference on ophiolites. Geotimes, 17: 24-25.

Nicolas A., 1989. Structures of ophiolites and dynamics of oceanic lithosphere. Kluwer, Dordrecht, 367 pp.

Dobretsov N.L., Moldavantsev Y.E., Kazak A.P., Ponomareva L.G., Savelieva G.N. and Saveliev A.A., 1977. Petrology and metamorphism of ancient ophiolites (examples from the Polar Urals and West Sayan). Nauka, Novosibirsk. (in Russian).

D'Orazio M. and Tonarini S., 1997. Simultaneous determination of neodymium and samarium in silicate rocks and minerals by isotope dilution inductively coupled plasma mass spectrometry: results on twenty geochemical reference samples. Anal. Chim. Acta, 351: 325-335.

Lupanova N.P. and Markin V.V., 1964. Greenstone sequences in the Sob-Voykar Synclinorium (Eastern Slope of the Polar Urals). Nauka, Moscow, 175 pp. (in Russian).

Pearce J.A., Lippard S.J. and Roberts S., 1985. Characteristics and tectonic significance of supra-subduction zone ophiolites. In: B.P. Kokelaar and M.F. Howells (Eds.), Marginal basin geology. Geol. Soc. London Spec. Publ., 16: 77-94.

Perfiliev A.S., 1979. The Uralian Geosyncline and the development of the Earth's crust. Nauka, Moscow, 188 pp. (in Russian).

Saveliev A.A., 1997. Ultramafic-gabbroic associations in the Voykar-Syn'ya Ophiolitic Massif (the Polar Urals). Geotectonics, 31 (1): 43-53.

Saveliev A.A. and Samygin S.G., 1979. Ophiolite allochthons of the Subarctic and Polar Urals. In: Tectonic evolution of the Earth's crust and faults. Nauka, Moscow, p. 9-30 (in Russian).

Saveliev A.A. and Savelieva G.N., 1977. Ophiolites of the Voykar-Syn'insk massif (Polar Urals). Geotectonics, 11 (6): 427-437.

Savelieva G.N., 1987. Gabbro-ultrabasite assemblages of Uralian ophiolites and their analogues in the recent oceanic crust. Nauka, Moscow, 242 pp. (in Russian).

Savelieva G.N. and Nesbitt R.W., 1996. A synthesis of the stratigraphic and tectonic setting of the Uralian ophiolites. J. Geol. Soc. London, 153: 525-537.

Savelieva G.N. and Saveliev A.A., 1992. Relationship between peridotites and gabbroic sequences in the ophiolites of the Urals and the Lesser Caucasus. Ofioliti, 17 (1): 117-138.

Sharma M., Wasserburg G.J., Papanastassiou D.A., Quick J.E., Sharkov E.V. and Laz'ko E.E., 1995. High $^{143}Nd/^{144}Nd$ in extremely depleted mantle rocks. Earth Planet. Sci. Lett., 135: 101-114.

Sun S.S. and McDonough W.F., 1989. Chemical and isotopic systematics of oceanic basalts: implications for mantle composition and processes. In: A.D. Saunders and M.J. Norry (Eds.), Magmatism in the ocean basins. Geol. Soc. London Spec. Publ., 42: 313-345.

Sun S.S., Nesbitt R.W. and Sharaskin A.Ya., 1979. Geochemical characteristics of mid-oceanic ridge basalts. Earth Planet. Sci. Lett., 44: 119-138.

Yazeva R.G. and Bochkarev V.V., 1984. The Voykar Volcano-Plutonic Belt. Ural. Nauch. Centre USSR, Sverdlovsk. (in Russian).

Received, March 3, 1999
Accepted, May 24, 1999